第 34 卷 第 3 期
2017 年 9 月

原 子 核 物 理 评 论
Nuclear Physics Review

Vol. 34, No. 3
Sep., 2017

Article ID: 1007-4627(2017) 03-0392-11

Towards a Relativistic Formulation of Baryon-baryon Interactions in Chiral Perturbation Theory

REN Xiulei[1], LI Kaiwen[2], GENG Lisheng[2,3,†]

(*1. State Key Laboratory of Nuclear Physics and Technology, School of Physics, Peking University, Beijing 100871, China;*
2. School of Physics and Nuclear Energy Engineering & International Research Center for Nuclei and Particles in the Cosmos, Beihang University, Beijing 100191, China;
3. Beijing Key Laboratory of Advanced Nuclear Materials and Physics, Beihang University, Beijing 100191, China)

Abstract: In this paper, we report on two recent studies of relativistic nucleon-nucleon and hyperon-nucleon interactions in covariant chiral perturbation theory, where they are constructed up to leading order. The relevant unknown low energy constants are fixed by fitting to the nucleon-nucleon and hyperon-nucleon scattering data. It is shown that these interactions can describe the scattering data with a quality similar to their next-to-leading order non-relativistic counterparts. These studies show that it is technically feasible to construct relativist baryon-baryon interactions, and in addition, after further refinements, these interactions may provide important inputs to *ab initio* relativistic nuclear structure and reaction studies and help improve our understanding of low energy strong interactions.

Key words: nucleon-nucleon interaction; hyperon-nucleon interaction; covariant chiral perturbation theory

CLC number: O572.3 **Document code:** A **DOI:** 10.11804/NuclPhysRev.34.03.392

1 Introduction

The nuclear force is one of the most important inputs to microscopic nuclear structure and reaction studies. It is responsible for holding nucleons together to form nuclei. As a residual force of the strong interaction, it can in principle be derived from the underlying theory of the strong interaction, Quantum Chromo Dynamics (QCD). However, because of the two peculiar properties of QCD, confinement and asymptotic freedom, QCD becomes non-perturbative at the low energy region of nuclear physics interest and, as a result, a direct derivation of realistic nuclear forces from first principles has only become possible in recent years via lattice QCD simulations[1, 2]. In Lattice 2016, the HAL QCD collaboration has reported on their preliminary results of baryon-baryon (BB) interactions at the (almost) physical point[3–5].

The original microscopic understanding of the nucleon-nucleon (NN) interaction was first proposed by Yukawa, namely, it is mediated by meson exchanges[6]. Ever since, the idea has been rather popular and successful phenomenologically. Nowadays, there are a variety of formulations of the nuclear force based on such a picture, such as the high-precision nuclear potentials, Reid93[7], Argonne V_{18}[8], (CD-)Bonn[9, 10]. In a similar way, one can derive hyperon-nucleon (YN) and hyperon-hyperon (YY) interactions as well, such as NSC97a-f[11]and Jülich 04[12]. These interactions serve as important inputs to (hyper)nuclear structure and reaction studies. Nonetheless, the connection of these phenomenological potentials to QCD is not very transparent.

The next advancement is the derivation of the nuclear force using chiral perturbation theory (ChPT), which is an effective field theory of low-energy QCD and provides a model independent way to study strong-interaction physics[13]. In 1990s, Weinberg proposed that one can derive the nuclear force from ChPT[14, 15]. The so-obtained chiral nuclear forces, based on a consistent power counting scheme, can be systematically improved by going to higher orders in terms of exter-

Received date: 19 Mar. 2017; **Revised date:** 20 May 2017
Foundation item: National Natural Science Foundation of China (11375024, 11522539, 11335002, 11621131001); China Postdoctoral Science Foundation (2016M600845, 2017T100008)
Biography: REN Xiulei(1987–), male, Jining, Shandong, Ph.D., working on theoretical nuclear physics; E-mail: xiulei.ren@pku.edu.cn.
† **Corresponding author:** GENG Lisheng, E-mail: lisheng.geng@buaa.edu.cn.

nal momenta (of the nucleons) and light quark masses. Three- and four-body interactions can be constructed on the same footing. In recent years, chiral nuclear forces have been constructed up to next-to-next-to-next-to-next-to-leading order (N^4LO) and can describe the NN scattering data with a $\chi^2/\text{datum} \lesssim 1$[16–21]. In the past decade, the Weinberg approach has been generalized to study antinucleon-nucleon[22, 23], YN and YY interactions[24–29]. Unlike the NN case, the chiral YN and YY interactions have only been formulated up to next-to-leading order (NLO).

The current studies of chiral forces are all based on non-relativistic (NR) chiral perturbation theory and relativistic effects are either discarded or treated perturbatively. On the other hand, relativistic effects are known to play an important role in understanding the fine structures of atoms/molecules[30] and nuclei[31], both of which are conventionally considered as typical low-energy and non-relativistic systems. Although because of their simplicity, NR approaches are still routinely used in modern studies, the dynamical relativistic effects, such as the appearance of antifermions, their spin and the resulting spin-orbit interactions, play a key role in understanding certain properties of finite nuclei, such as the origin of pseudospin symmetry[32]. Furthermore, relativistic effects at the hadronic level have been shown to play an important role as well, by the successful applications of covariant chiral perturbation theory in the one-baryon sector[33–38] and heavy-light systems[39–42].

Motivated by the successes of relativistic formulations in atomic/molecular, nuclear and hadronic systems and in response to the demand in *ab initio* relativistic nuclear structure studies[43, 44], we proposed to study the chiral BB interactions in the framework of covariant chiral perturbation theory. As a first step, we constructed the NN and YN interactions at leading order (LO) and made comparisons with their NR counterparts. The main results will be given in Sec. 3 and Sec. 4, respectively, while more details can be found in Refs. [45, 46].

2 Definition of relativistic baryon-baryon potentials

A potential is often understood as a quantity used in the non-relativistic Schrodinger/Lippmann-Schwinger equations. Since our purpose is to construct relativistic baryon-baryon potentials, it is worthy clarifying the definition of potentials from a field-theoretical point of view[47, 48], especially in the framework of covariant chiral perturbation theory.

Because of the non-perturbative nature of baryon-baryon interactions, in relativistic elastic scattering, one has to resort to the Bethe-Salpeter (BS) equation, which reads, *e.g.* for nucleon-nucleon scattering,

$$\mathcal{T}(p',p|W) = \mathcal{A}(p',p|W) + \int \frac{\mathrm{d}^4k}{(2\pi^4)} \mathcal{A}(p',k|W) G(k|W) T(k,p|W), \tag{1}$$

where p (p') is the initial (final) relative four-momentum in the center-of-mass system, and $W = (\sqrt{s}/2, \mathbf{0})$ is half of the total four-momentum with the total energy $\sqrt{s} = 2E_p = 2E_{p'}$ and $E_p = \sqrt{\boldsymbol{p}^2 + m_{\mathrm{N}}^2}$. $\mathcal{T}$ denotes the invariant amplitude, $\mathcal{A}$ is the interaction kernel consisting of all irreducible diagrams appearing in covariant ChPT. G represents the free two-nucleon Green function. However, because of both formal and practical considerations, one often uses a three-dimensional reduction of the BS equation in practice, such as the Blankenbecler-Sugar equation[49], the Thompson equation[50], the Kadyshevsky equation[51], or the Gross equation[52]. In the present work, following Refs. [53, 54], we chose to use the Kadyshevsky equation,

$$T(\boldsymbol{p}',\boldsymbol{p}) = V(\boldsymbol{p}',\boldsymbol{p}) + \int \frac{\mathrm{d}^3k}{(2\pi)^3} \times V(\boldsymbol{p}',\boldsymbol{k}) \frac{m_{\mathrm{N}}^2}{2E_k^2} \frac{1}{E_p - E_k + \mathrm{i}\epsilon} T(\boldsymbol{k},\boldsymbol{p}). \tag{2}$$

After integrating out the time component k_0 of the BS equation and sandwiching it between the nucleon Dirac spinors, we obtain the relativistic potential, V, appearing in the above equation,

$$V(\boldsymbol{p}',\boldsymbol{p}) = \bar{u}(\boldsymbol{p}',s_1)\bar{u}(-\boldsymbol{p}',s_2) \times \mathcal{V}[p_0' = E_{p'} - 1/2\sqrt{s}, \boldsymbol{p}'; p_0 = E_p - 1/2\sqrt{s}, \boldsymbol{p}|W] \times u(\boldsymbol{p},s_1) u(\boldsymbol{p}',s_2), \tag{3}$$

with the effective interaction kernel $\mathcal{V}$ perturbatively calculated via

$$\mathcal{V}^{(0)} = \mathcal{A}^{(0)}, \quad \mathcal{V}^{(2)} = \mathcal{A}^{(2)} + \mathcal{A}^{(0)}(G-g)\mathcal{A}^{(0)}, \tag{4}$$

and so on, in covariant ChPT.

3 Relativistic chiral nucleon-nucleon interactions

In Ref. [45], we proposed a covariant power counting scheme to derive the relativistic chiral nuclear force defined above. Under this power counting, we retain the full form of the Dirac spinors, *i.e.*,

$$u(\boldsymbol{p},s) = N_{\mathrm{p}} \begin{pmatrix} 1 \\ \frac{\boldsymbol{\sigma}\cdot\boldsymbol{p}}{\epsilon_p} \end{pmatrix} \chi_s, \quad N_{\mathrm{p}} = \sqrt{\frac{\epsilon_p}{2M_{\mathrm{N}}}}, \tag{5}$$

with $\epsilon_{\rm p} = E_{\rm p} + M_{\rm N}$. The chiral dimension of a Feynman diagram is determined by

$$n_\chi = 4L - 2N_\pi - N_{\rm n} + \sum_k k V_k, \tag{6}$$

where L is the number of loops, N_π the number of internal pion lines, $N_{\rm n}$ the number of internal nucleon lines, and V_k the vertices of chiral dimension k. In the covariant power counting, the expansion parameters in constructing V_k are the external nucleon three momenta and light quark masses, which are the same as those in the one-baryon sector. It should be mentioned that such power counting schemes are well defined in the $\pi\pi$ and πN sectors, but not in the NN sector. Here, we follow the strategies outlined in Refs. [55, 56]. In addition, the Dirac spinors are treated as one entity and the small components are retained, different from the NR approach.

According to the above power counting, at leading order one needs to compute the Feynman diagrams shown in Fig. 1. The relevant Lagrangians are

$$\mathcal{L}_{\rm eff.} = \mathcal{L}^{(2)}_{\pi\pi} + \mathcal{L}^{(1)}_{\pi{\rm N}} + \mathcal{L}^{(0)}_{\rm NN}, \tag{7}$$

where the superscript denotes the chiral dimension. The lowest order $\pi\pi$, πN and NN Lagrangians read,

$$\mathcal{L}^{(2)}_{\pi\pi} = \frac{f_\pi^2}{4}{\rm Tr}\left[\partial_\mu U \partial^\mu U^\dagger + (U + U^\dagger) m_\pi^2\right], \tag{8}$$

$$\mathcal{L}^{(1)}_{\pi{\rm N}} = \bar\Psi\left[{\rm i}\not{D} - M_N + \frac{g_A}{2}\gamma^\mu\gamma_5 u_\mu\right]\Psi, \tag{9}$$

$$\begin{aligned}\mathcal{L}^{(0)}_{\rm NN} = \frac{1}{2}\big[&C_S(\bar\Psi\Psi)(\bar\Psi\Psi) + C_A(\bar\Psi\gamma_5\Psi)(\bar\Psi\gamma_5\Psi) + \\ &C_V(\bar\Psi\gamma_\mu\Psi)(\bar\Psi\gamma^\mu\Psi) + \\ &C_{AV}(\bar\Psi\gamma_\mu\gamma_5\Psi)(\bar\Psi\gamma^\mu\gamma_5\Psi) + \\ &C_T(\bar\Psi\sigma_{\mu\nu}\Psi)(\bar\Psi\sigma^{\mu\nu}\Psi)\big],\end{aligned} \tag{10}$$

where the pion decay constant $f_\pi = 92.4$ MeV, the axial vector coupling $g_A = 1.267$, and $C_{S,A,V,AV,T}$ are low-energy constants (LECs). We note that the relativistic chiral Lagrangians for nucleon-nucleon interactions have been constructed up to leading order by a number of groups[24, 56]. There are also attempts at the next-to-leading order[55, 57]. Nonetheless, further efforts are still needed to have a systematic power counting in the relativistic case at NLO and beyond.

As shown in Fig. 1, the LO relativistic chiral nuclear interaction includes four-nucleon contact (CTP) and one-pion-exchange potentials (OPEP),

$$V^{\rm NN}_{\rm LO} = V^{\rm NN}_{\rm CTP} + V^{\rm NN}_{\rm OPEP}, \tag{11}$$

with

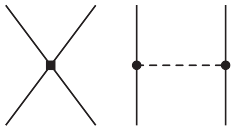

Fig. 1 Feynman diagrams contributing to the LO relativistic chiral force. Solid lines represent nucleons and the dashed line denotes the pion.

$$\begin{aligned}&V_{\rm CTP}(\boldsymbol{p}',\boldsymbol{p}) = \\ &C_S\left(\bar u(\boldsymbol{p}',s_1')u(\boldsymbol{p},s_1)\right)\left(\bar u(-\boldsymbol{p}',s_2')u(-\boldsymbol{p},s_2)\right) + \\ &C_A\left(\bar u(\boldsymbol{p}',s_1')\gamma_5 u(\boldsymbol{p},s_1)\right)\left(\bar u(-\boldsymbol{p}',s_2')\gamma_5 u(-\boldsymbol{p},s_2)\right) + \\ &C_V\left(\bar u(\boldsymbol{p}',s_1')\gamma_\mu u(\boldsymbol{p},s_1)\right)\left(\bar u(-\boldsymbol{p}',s_2')\gamma^\mu u(-\boldsymbol{p},s_2)\right) + \\ &C_{AV}\left(\bar u(\boldsymbol{p}',s_1')\gamma_\mu\gamma_5 u(\boldsymbol{p},s_1)\right)\times \\ &(\bar u(-\boldsymbol{p}',s_2')\gamma^\mu\gamma_5 u(-\boldsymbol{p},s_2)) + \\ &C_T\left(\bar u(\boldsymbol{p}',s_1')\sigma_{\mu\nu}u(\boldsymbol{p},s_1)\right)\times \\ &\left(\bar u(-\boldsymbol{p}',s_2')\sigma^{\mu\nu}u(-\boldsymbol{p},s_2)\right)\ ,\end{aligned} \tag{12}$$

and

$$\begin{aligned}V_{\rm OPEP}(\boldsymbol{p}',\boldsymbol{p}) = -\frac{g_A^2}{4f_\pi^2}&\frac{1}{(E_{p'}-E_p)^2-(\boldsymbol{p}'-\boldsymbol{p})^2-m_\pi^2}\times \\ &\left[\bar u(\boldsymbol{p}',s_1')\boldsymbol{\tau}_1\gamma^\mu\gamma_5 q_\mu u(\boldsymbol{p},s_1)\right]\cdot \\ &\left[\bar u(-\boldsymbol{p}',s_2')\boldsymbol{\tau}_2\gamma^\nu\gamma_5 q_\nu u(-\boldsymbol{p},s_2)\right]\ ,\end{aligned} \tag{13}$$

where q represents the four momentum transfer $q = (E_{p'} - E_p, \boldsymbol{p}' - \boldsymbol{p})$ and $\boldsymbol{\tau}$ are the isospin Pauli matrices. It should be noted that the retardation effect of OPEP is self-consistently included, consistent with the assumption of the Kadyshevsky equation.

Rewriting the LO potential in terms of the Pauli operators and three momenta, it is easy to see that $V^{\rm NN}_{\rm LO}$ contains all the six allowed spin operators, in contrast with the non-relativistic LO chiral potential, which only consists of the central, spin-spin and tensor operators.

Next, we perform partial wave decomposition of the chiral potential in the $|LSJ\rangle$ basis and connect them to experimental observables. First, one calculates the matrix elements of $V^{\rm NN}_{\rm LO}$ in the helicity basis, then rotates them to the total angular momentum space $|JM\rangle$, and finally, transforms them to the $|LSJ\rangle$ representation. We note that the relativistic contact terms contribute to all the $J \leqslant 1$ partial waves and the relativistic corrections to the OPEP are largely suppressed.

As mentioned before, in the present work, we chose to use the Kadyshevsky equation*, which reads in the LSJ basis,

$$T^{SJ}_{L',L}(\boldsymbol{p}',\boldsymbol{p}) = V^{SJ}_{L',L}(\boldsymbol{p}',\boldsymbol{p}) +$$

*We checked that using the Blankenbecler-Sugar equation to obtain the scattering amplitude does not change our results in any significant way.

$$\sum_{L''}\int_0^{+\infty}\frac{\boldsymbol{k}^2\mathrm{d}k}{(2\pi)^3}V^{SJ}_{L',L}(\boldsymbol{p}',\boldsymbol{k})\frac{M_{\mathrm{N}}^2}{2E_k^2}\times \frac{1}{E_p-E_k+\mathrm{i}\epsilon}T^{SJ}_{L'',L}(\boldsymbol{k},\boldsymbol{p}). \tag{14}$$

Furthermore, to avoid ultraviolet divergence, we regularize the potential in Eq. (14) with a form factor. Here, we choose the commonly used separable cutoff function[59],

$$V_{\mathrm{LO}}\to V_{\mathrm{LO}}^{\mathrm{Reg.}}=V_{\mathrm{LO}}\ \exp\left(\frac{-\boldsymbol{p}^{2n}-\boldsymbol{p}'^{2n}}{\Lambda^{2n}}\right), \tag{15}$$

with $n=2$. One should note that such a form factor is not covariant, but using the same cutoff function as that used in the NR approach allows us to make a direct comparison between the relativistic and NR approaches.**

In order to determine the five unknown LECs, we need to fit to the NN scattering phase shifts. We choose the neutron-proton phase shifts from the Nijmegen93 partial wave analysis[58] with laboratory kinetic energy $E_{\mathrm{lab.}}\leqslant 100$ MeV. The momentum cutoff Λ is varied from 500 MeV to 1 000 MeV. We found that the best fitted result is located at $\Lambda=750$ MeV with $\tilde{\chi}^2/\mathrm{d.o.f.}\sim 2.0$, and the corresponding description of phase shifts is presented in Fig. 2. For the sake of comparison, the results of the LO and NLO non-relativistic chiral force from Ref. [59] are also shown.

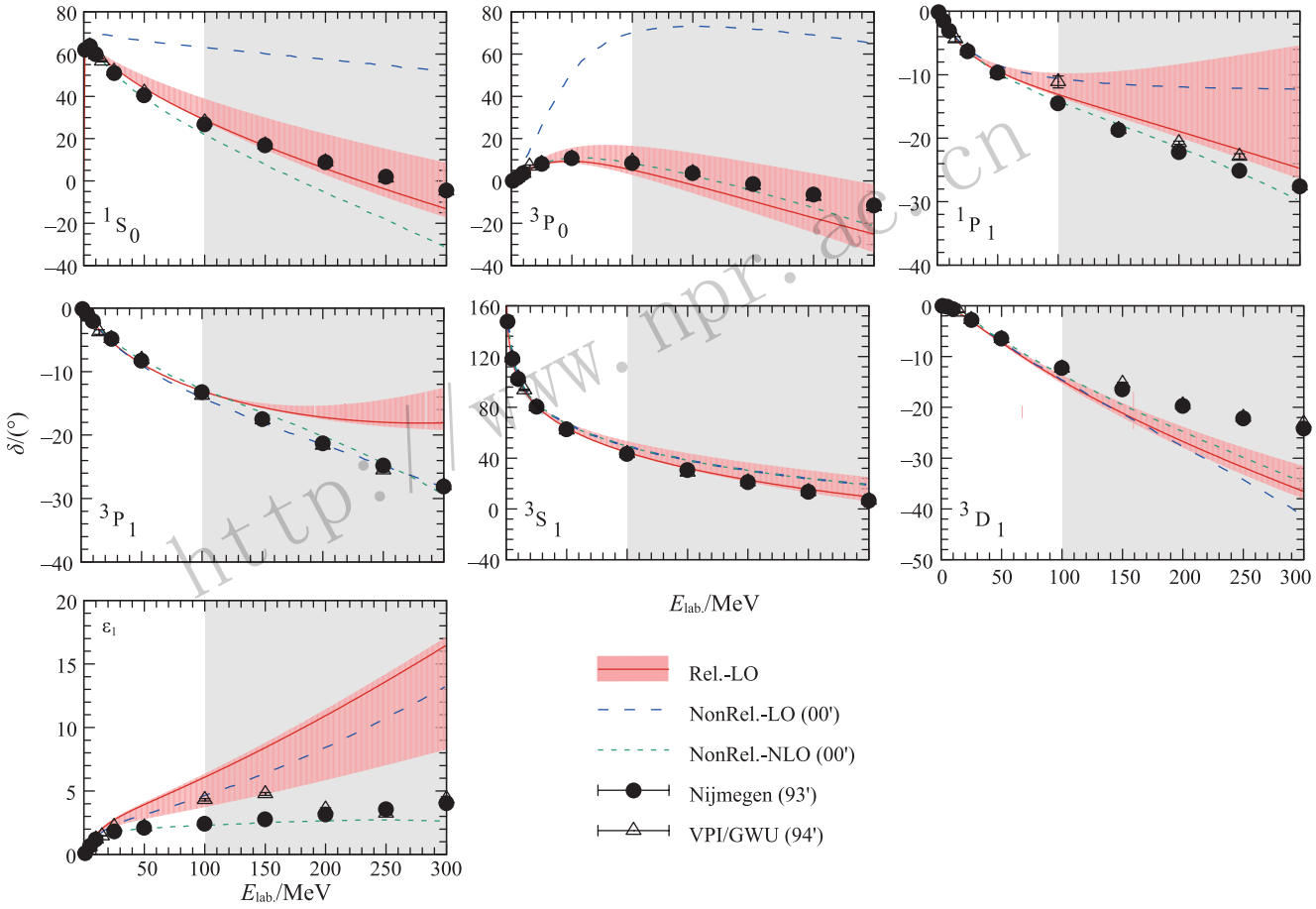

Fig. 2　(color online) Comparison of theoretical and experimental neutron-proton phase shifts for $J\leqslant 1$. The red solid lines represent the results of the LO relativistic potential, while the dashed and dotted lines denote the LO and NLO non-relativistic results[59]. The red bands are the relativistic results with the cutoff ranging from 500 MeV to 1 000 MeV. Solid dots and open triangles are the np phase shifts of Nijmegen[58] and VPI/GWU[60]. The gray backgrounds denote the energy regions where the theoretical results are predictions. The figure is taken from Ref. [45].

** We realized that there exists a covariant but separable cutoff function of the following form,

$$V_{\mathrm{LO}}\to V_{\mathrm{LO}}^{\mathrm{Reg.}}=\exp\left[-\left(\frac{p^2-m_{\mathrm{N}}^2}{\Lambda^2}\right)\right]\ V_{\mathrm{LO}}\ \exp\left[-\left(\frac{p'^2-m_{\mathrm{N}}^2}{\Lambda^2}\right)\right]. \tag{16}$$

Preliminary studies show that using such a cutoff function yields slightly better fits compared to what shown in Ref. [45], but the results remain qualitatively similar. More details will be reported in a forthcoming publication.

Furthermore, the variations from the best fit with the cutoff ranging from 500 MeV to 1 000 MeV are shown as the red bands in Fig. 2. The covariant LO results can better describe the $^1S_0$ and $^3P_0$ phase shifts than the corresponding NR ones. They are quantitatively similar to the NLO NR ones. It can be seen that the variation of the cutoff does not change qualitatively the overall picture. On the other hand, for the five $J=1$ phase shifts, the relativistic results are almost the same as the non-relativistic ones.

In Fig. 3, we show the description of the $J=2$ phase shifts, where only one-pion-exchange diagrams contribute. Following the same strategies, we give the relativistic results with $\Lambda=750$ MeV as central values and the variation bands are obtained by varying the cutoff from 500 MeV to 1000 MeV. For the sake of comparison, the LO non-relativistic results of Ref. [59] are also shown. One can see that they are almost the same, because the relativistic corrections of the OPEP are largely suppressed.

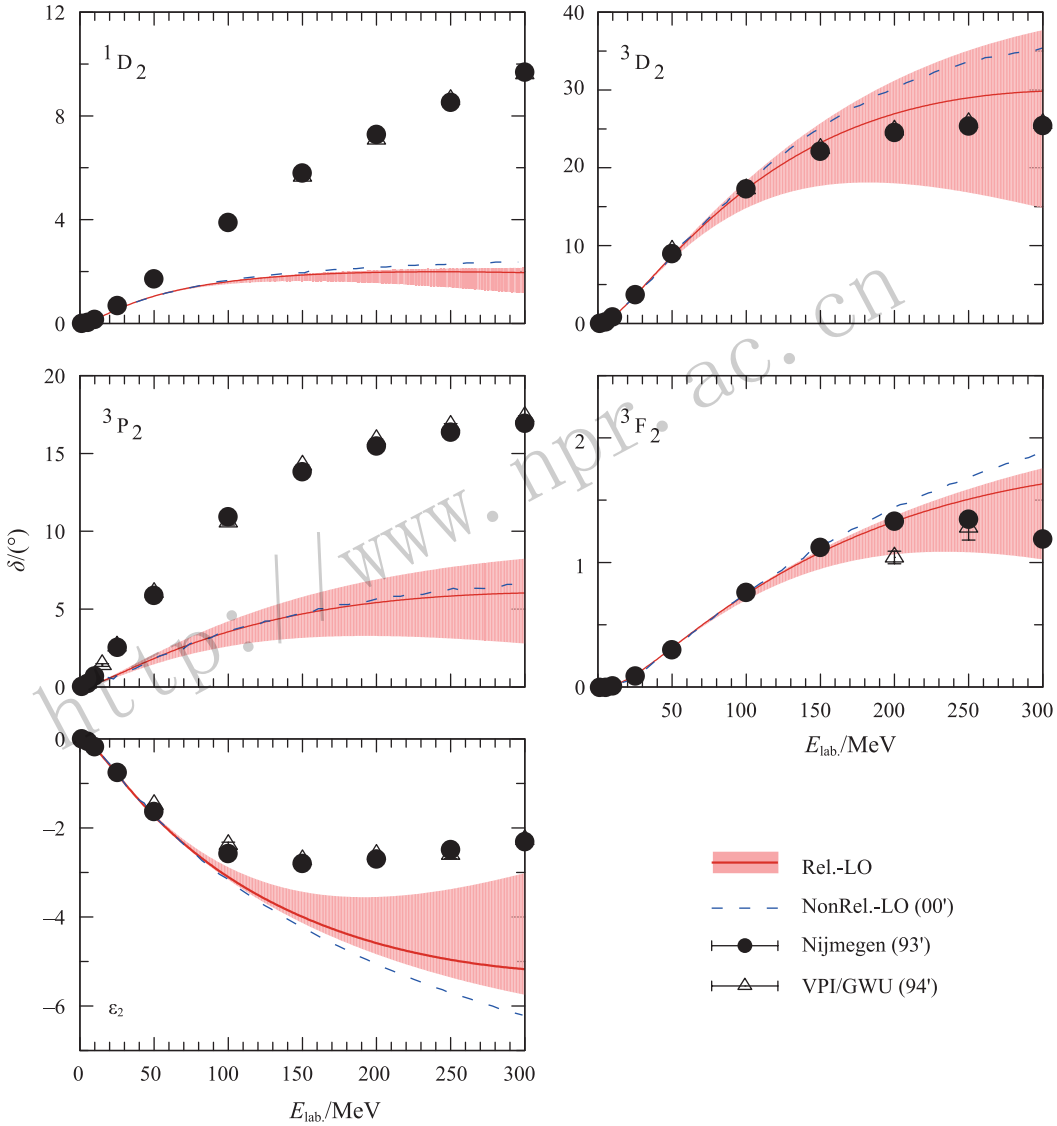

Fig. 3 (color online) Neutron-proton phase shifts for $J=2$. The notations are the same as Fig. 2. The figure is taken from Ref.[45].

4 Relativistic chiral hyperon-nucleon interaction

We have extended the covariant power counting scheme to the YN sector and constructed the strangeness $S=-1$ YN interaction up to LO in Ref. [46]. The Lagrangians for the contact terms (CT) and the one-pseudoscalar-meson-exchange potential (OPME) read

$$\mathcal{L}_{\rm CT}=\frac{\tilde{C}_i^1}{2}\ {\rm tr}\left(\bar{B}_a\bar{B}_b(\Gamma_i B)_b(\Gamma_i B)_a\right)+$$

$$\frac{\tilde{C}_i^2}{2}\,\mathrm{tr}\left(\bar{B}_a(\Gamma_i B)_a\bar{B}_b(\Gamma_i B)_b\right)+\frac{\tilde{C}_i^3}{2}\,\mathrm{tr}\left(\bar{B}_a(\Gamma_i B)_a\right)\mathrm{tr}\left(\bar{B}_b(\Gamma_i B)_b\right), \tag{17}$$

$$\mathcal{L}_{\mathrm{MB}}^{(1)}=\mathrm{tr}\left(\bar{B}\left(\mathrm{i}\gamma_\mu D^\mu-M_B\right)B-\frac{D}{2}\bar{B}\gamma^\mu\gamma_5\{u_\mu,B\}-\frac{F}{2}\bar{B}\gamma_\mu\gamma_5[u_\mu,B]\right). \tag{18}$$

The potential can be symbolically expressed as

$$V_{\mathrm{LO}}^{\mathrm{BB}'}=V_{\mathrm{CT}}^{\mathrm{BB}'}+V_{\mathrm{OPME}}^{\mathrm{BB}'}. \tag{19}$$

The contact terms are derived assuming SU(3) symmetry[61]. The OPME potential reads

$$V_{\mathrm{OPME}}^{\mathrm{BB}'}=-N_{B_1B_3\phi}N_{B_2B_4\phi}\mathcal{I}_{B_1B_2\to B_3B_4}\times\frac{(\bar{u}_3\gamma^\mu\gamma_5 q_\mu u_1)(\bar{u}_4\gamma^\nu\gamma_5 q_\nu u_2)}{q^2-m^2}, \tag{20}$$

where the $SU(3)$ coefficient $N_{\mathrm{BB}'\phi}$ and isospin factor $\mathcal{I}_{B_1B_2\to B_3B_4}$ can be found in, *e.g.*, Refs. [24, 61]. Note that $SU(3)$ symmetry is broken due to the mass difference of the exchanged mesons. The corresponding Feynman diagrams for the strangeness $S=-1$ ΛN–ΣN system are shown in Figs. 4∼5.

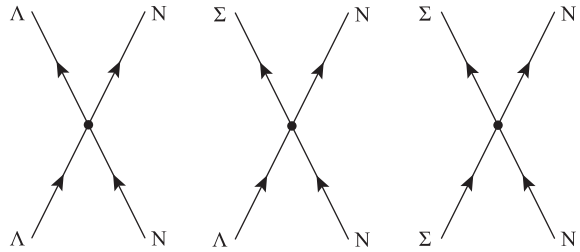

Fig. 4　Nonderivative four baryon contact terms in the ΛN − ΣN system.

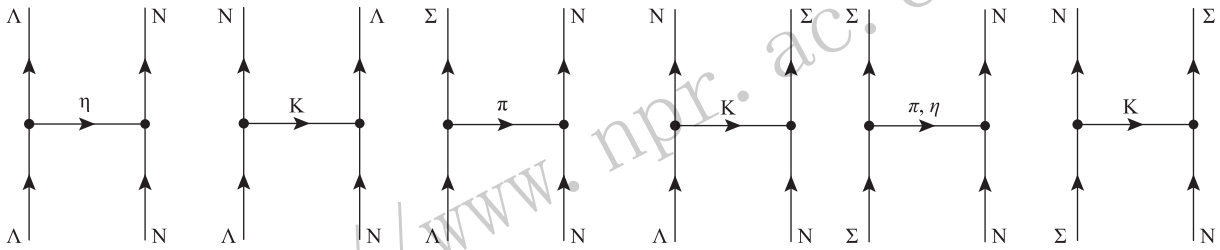

Fig. 5　One-pseudoscalar-meson exchange diagrams in the ΛN − ΣN system.

Following the same procedure as in the NN case, one can perform partial wave decompositions of the LO YN potential and obtain $V_{\mathrm{LO}}^{\mathrm{YN}}$ in the $|LSJ\rangle$ basis. After iteration of the partial wave potential in the coupled-channel Kadyshevsky equation,

$$T_{\rho\rho'}^{\nu\nu',J}(\boldsymbol{p}',\boldsymbol{p};\sqrt{s})=V_{\rho\rho'}^{\nu\nu',J}(\boldsymbol{p}',\boldsymbol{p})+\sum_{\rho'',\nu''}\int_0^\infty\frac{\mathrm{d}p''p''^2}{(2\pi)^3}\times\frac{M_{B_{1,\nu''}}M_{B_{2,\nu''}}\;V_{\rho\rho''}^{\nu\nu'',J}(\boldsymbol{p}',\boldsymbol{p}'')\;T_{\rho''\rho'}^{\nu''\nu',J}(\boldsymbol{p}'',\boldsymbol{p};\sqrt{s})}{E_{1,\nu''}E_{2,\nu''}\left(\sqrt{s}-E_{1,\nu''}-E_{2,\nu''}+\mathrm{i}\epsilon\right)}, \tag{21}$$

one can obtain the scattering T-matrix. In Eq. (21), the potential needs also to be regularized to avoid ultraviolet divergence. We chose the Gaussian cutoff function Eq. (15) as in the NN case. Furthermore, in order to properly take into account the physical thresholds and the Coulomb force in charged channels, we solve the Kadyshevsky equation in particle basis. The Coulomb effects are treated with the Vincent-Phatak approach.

Among the 15 LECs in the Lagrangian of Eq. (16), it can be easily shown that there are only 12 independent LECs or equivalently 12 independent partial waves in the strangeness $S=-1$ sector.[¶] To do this, one can write down the following 12 partial wave potentials which are linear functions of the 12 LECs we introduced in Ref. [46].

$$V_{1S0}^{\Lambda\Lambda}=C_{1S0}^{\Lambda\Lambda}\left[1+(R_{\mathrm{p}}^{\Lambda\Lambda})^2(R_{\mathrm{p}'}^{\Lambda\Lambda})^2\right]+\hat{C}_{1S0}^{BB'}\left[(R_{\mathrm{p}}^{\Lambda\Lambda})^2+(R_{\mathrm{p}'}^{\Lambda\Lambda})^2\right],$$

$$V_{1S0}^{\Sigma\Sigma}=C_{1S0}^{\Sigma\Sigma}\left[1+(R_{\mathrm{p}}^{\Sigma\Sigma})^2(R_{\mathrm{p}'}^{\Sigma\Sigma})^2\right]+\hat{C}_{1S0}^{BB'}\left[(R_{\mathrm{p}}^{\Sigma\Sigma})^2+(R_{\mathrm{p}'}^{\Sigma\Sigma})^2\right],$$

$$V_{3P1}^{\Lambda\Lambda}=-\frac{4}{3}C_{3P1}^{\Lambda\Lambda}R_{\mathrm{p}}^{\Lambda\Lambda}R_{\mathrm{p}'}^{\Lambda\Lambda},$$

$$V_{3P1}^{\Sigma\Sigma}=-\frac{4}{3}C_{3P1}^{\Sigma\Sigma}R_{\mathrm{p}}^{\Sigma\Sigma}R_{\mathrm{p}'}^{\Sigma\Sigma},$$

$$V_{3P0}^{\Lambda\Lambda}=-2(-C_{1S0}^{\Lambda\Lambda}-\hat{C}_{1S0}^{\Lambda\Lambda}+2D_{3S1}^{\Lambda\Lambda}-2\hat{D}_{3S1}^{\Lambda\Lambda})R_{\mathrm{p}}^{\Lambda\Lambda}R_{\mathrm{p}'}^{\Lambda\Lambda},$$

$$V_{3P0}^{\Sigma\Sigma}=-2(-C_{1S0}^{\Sigma\Sigma}-\hat{C}_{1S0}^{\Sigma\Sigma}+2D_{3S1}^{\Sigma\Sigma}-2\hat{D}_{3S1}^{\Sigma\Sigma})R_{\mathrm{p}}^{\Sigma\Sigma}R_{\mathrm{p}'}^{\Sigma\Sigma},$$

¶ The other three LECs contribute exclusively to the strangeness $S=-2$ system.

$$
\begin{aligned}
V_{3S1}^{\Lambda\Lambda} &= C_{3S1}^{\Lambda\Lambda}\left[1+(R_{\rm p}^{\Lambda\Lambda})^2(R_{\rm p'}^{\Lambda\Lambda})^2\right]+\\
&\quad \hat{C}_{3S1}^{\Lambda\Lambda}\left[(R_{\rm p}^{\Lambda\Lambda})^2+(R_{\rm p'}^{\Lambda\Lambda})^2\right],\\
V_{3S1}^{\Sigma\Sigma} &= C_{3S1}^{\Sigma\Sigma}\left[1+(R_{\rm p}^{\Sigma\Sigma})^2(R_{\rm p'}^{\Sigma\Sigma})^2\right]+\\
&\quad \hat{C}_{3S1}^{\Sigma\Sigma}\left[(R_{\rm p}^{\Sigma\Sigma})^2+(R_{\rm p'}^{\Sigma\Sigma})^2\right],\\
V_{3S1}^{\Lambda\Sigma} &= C_{3S1}^{\Lambda\Sigma}\left[1+(R_{\rm p}^{\Lambda\Sigma})^2(R_{\rm p'}^{\Lambda\Sigma})^2\right]+\\
&\quad \hat{C}_{3S1}^{\Lambda\Sigma}\left[(R_{\rm p}^{\Lambda\Sigma})^2+(R_{\rm p'}^{\Lambda\Sigma})^2\right],\\
V_{1P1}^{\Lambda\Lambda} &= -\frac{2}{3}(C_{3S1}^{\Lambda\Lambda}-\hat{C}_{3S1}^{\Lambda\Lambda})R_{\rm p}^{\Lambda\Lambda}R_{\rm p'}^{\Lambda\Lambda},\\
V_{1P1}^{\Sigma\Sigma} &= -\frac{2}{3}(C_{3S1}^{\Sigma\Sigma}-\hat{C}_{3S1}^{\Sigma\Sigma})R_{\rm p}^{\Sigma\Sigma}R_{\rm p'}^{\Sigma\Sigma},\\
V_{1P1}^{\Lambda\Sigma} &= -\frac{2}{3}(C_{3S1}^{\Lambda\Sigma}-\hat{C}_{3S1}^{\Lambda\Sigma})R_{\rm p}^{\Lambda\Sigma}R_{\rm p'}^{\Lambda\Sigma}\ ,
\end{aligned}
\tag{22}
$$

where

$$
\begin{aligned}
D_{3S1}^{\Lambda\Lambda} &= \frac{1}{18}\left(17C_{3S1}^{\Lambda\Lambda}+15C_{3S1}^{\Lambda\Sigma}+C_{3S1}^{\Sigma\Sigma}\right),\\
\hat{D}_{3S1}^{\Lambda\Lambda} &= \frac{1}{18}\left(17\hat{C}_{3S1}^{\Lambda\Lambda}+15\hat{C}_{3S1}^{\Lambda\Sigma}+\hat{C}_{3S1}^{\Sigma\Sigma}\right),\\
D_{3S1}^{\Sigma\Sigma} &= C_{3S1}^{\Lambda\Lambda}+C_{3S1}^{\Lambda\Sigma},\\
\hat{D}_{3S1}^{\Sigma\Sigma} &= \hat{C}_{3S1}^{\Lambda\Lambda}+\hat{C}_{3S1}^{\Lambda\Sigma}\ .
\end{aligned}
\tag{23}
$$

One can easily check that this set of equations has a unique solution, which means that they are linearly independent. The remaining potentials, namely the ${}^3S_1-{}^3D_1$ mixing and ${}^3D_1$, can be expressed in terms of $V_{3S1}^{\rm BB'}$ and $V_{1P1}^{\rm BB'}$. The only other choice is to take those LECs in the ${}^1S_0$, ${}^3S_1$ and ${}^3P_0$ partial waves.

To determine the 12 unknown LECs, we performed a fit to the scarce low energy YN scattering data, which consist of 35 cross sections and a Σ^-p inelastic capture ratio at rest. We also took into account the S-wave scattering lengths of Λp and Σ^+p to further constrain the values of LECs. The cutoff scale Λ was varied from 500 to 850 MeV. The details of the fit can be found in Ref. [46].

The best fitted results are obtained at $\Lambda = 600$ MeV, with a $\chi^2 = 16.1$. The corresponding description of the experimental cross sections are presented in Fig. 6. For references, the results of two phenomenological potentials, NSC97f and Jülich04, and those of the LO NR chiral force are also shown. One can see that the relativistic results can reproduce the YN scattering data quite well.

Moreover, differential cross sections are also shown in Fig. 7. One can see that the theoretical predictions agree well with the experimental data within uncertainties, although they are not considered in the fits. S- and P-wave phase shifts of Λp and Σ^+p reactions are shown in Figs. 8∼9. One can see that the ${}^1S_0$ and ${}^3P_0$ phase shifts are quite different from those of the LO NR approach, but the ${}^3P_2$ phase shifts are similar, where only OPME terms contribute.

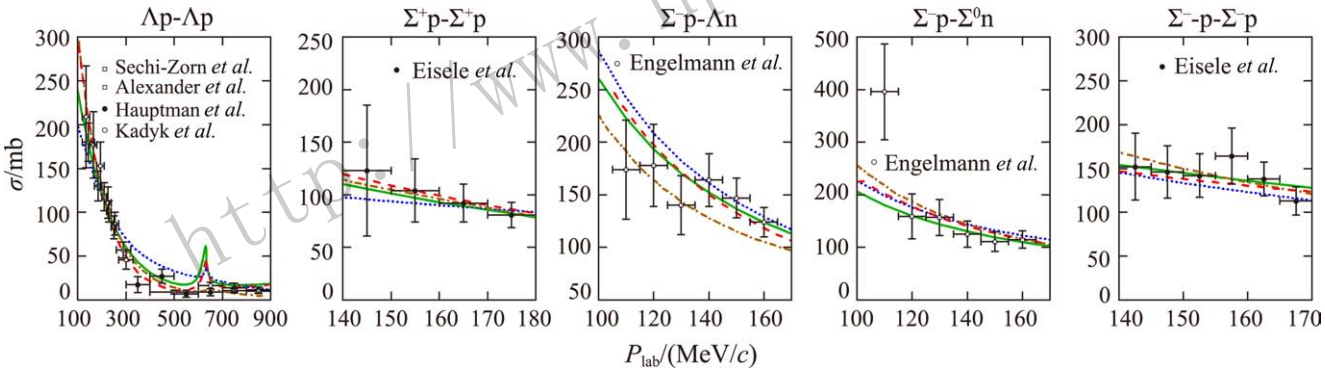

Fig. 6 (color online) Cross sections in the leading order relativistic χEFT approach (green solid lines) and NR approach (blue dotted lines)as functions of the laboratory momentum at $\Lambda_{\rm F} = 600$ MeV. For reference, the NSC97f[11] (red dash lines) and Jülich 04[12] (orange dashed-dotted lines) results are also shown. The figure is taken from Ref. [46].

Cutoff dependence of the fitted χ^2 is shown in Fig. 10, in comparison with the LO[24] and NLO[26] NR approach, and the approach in Refs. [53, 54] (denoted as the EG approach). The relativistic results are less sensitive to the cutoff variation, compared with the LO NR approach and the EG approach, and are comparable with the NLO NR approach. Similar to the NN case, the improvement mainly originates from the contact terms.

We have tried to describe the NN and YN data simultaneously and found that a simultaneous fit of NN and YN systems is impossible, similar to the NLO NR case[26]. This can be demonstrated in the following way. One can easily see that the LECs in the NN sector fixed by fitting to the Nijmegen partial wave analysis with $E_{\rm lab.} \leqslant 100$ MeV as described in Sec. 3 are quite different from the ones fixed by fitting to the scattering data described above. More specifically,

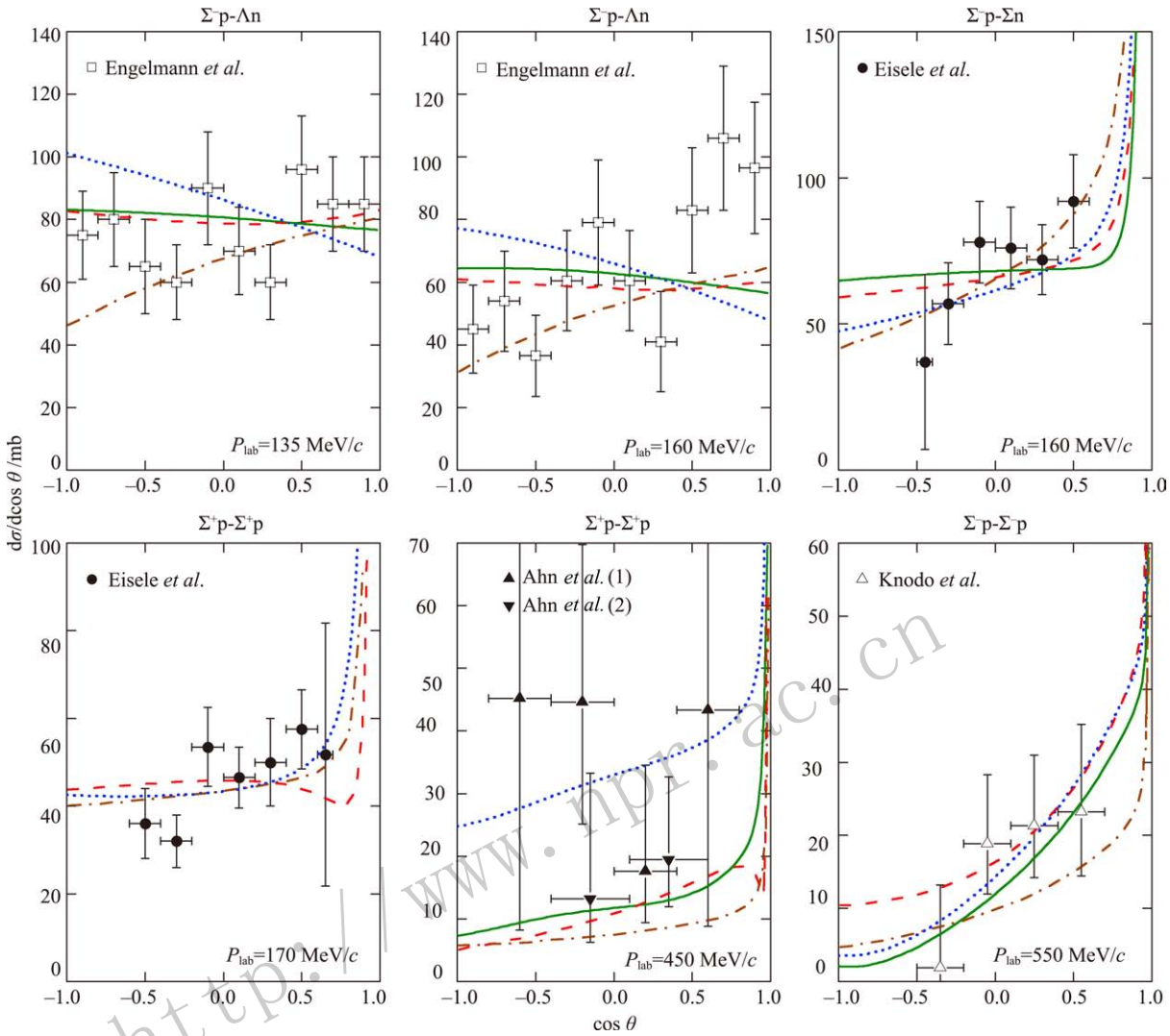

Fig. 7　(color online) Differential cross sections as a function of cosθ at various laboratory momenta $P_{\rm lab}$, where θ is the center-of-mass scattering angle. The notations are the same as Fig. 6. The figure is taken from Ref. [46].

YN the $^1S_0$ partial waves of NN ($I=1$) and ΣN($I=3/2$) share the same $SU(3)$ representation 27. As a result the contact terms should be the same for these two channels in the $SU(3)$ symmetric limit. However, we find that the $\Sigma^+p\to\Sigma^+p$ cross sections are largely overestimated with the LECs determined from the NN analysis, and even a near-threshold bound state appears. We conclude that $SU(3)$ symmetry breaking must be properly taken into account in order to describe the NN and YN scattering simultaneously.

5　Summary and perspectives

We proposed a new covariant power counting scheme to construct relativistic baryon-baryon (NN, YN, and YY) interactions based on covariant chiral perturbation theory. The NN and YN interactions were formulated up to leading order and it was shown that they can describe the NN and YN scattering data reasonably well, similar to the next-to-leading order non-relativistic ones. From an effective field theory of point of view, such a feature, namely, being able to describe experiments as relatively low order and with fewer low energy constants, is very welcome. Of course, more studies are needed to verify whether it will continue into higher orders.

In the near future, we would like to construct the relativistic chiral nuclear force up to next-to-next-to-leading order and determine the relevant low-energy constants by fitting to either NN phase shifts or scattering data directly. We expect to obtain a high precision chiral nuclear force for relativistic nuclear structure and reaction studies. In the mean time, we will extend the same framework to study YN and YY interactions. With the latest results from lattice QCD simulations, we can achieve a better determination of

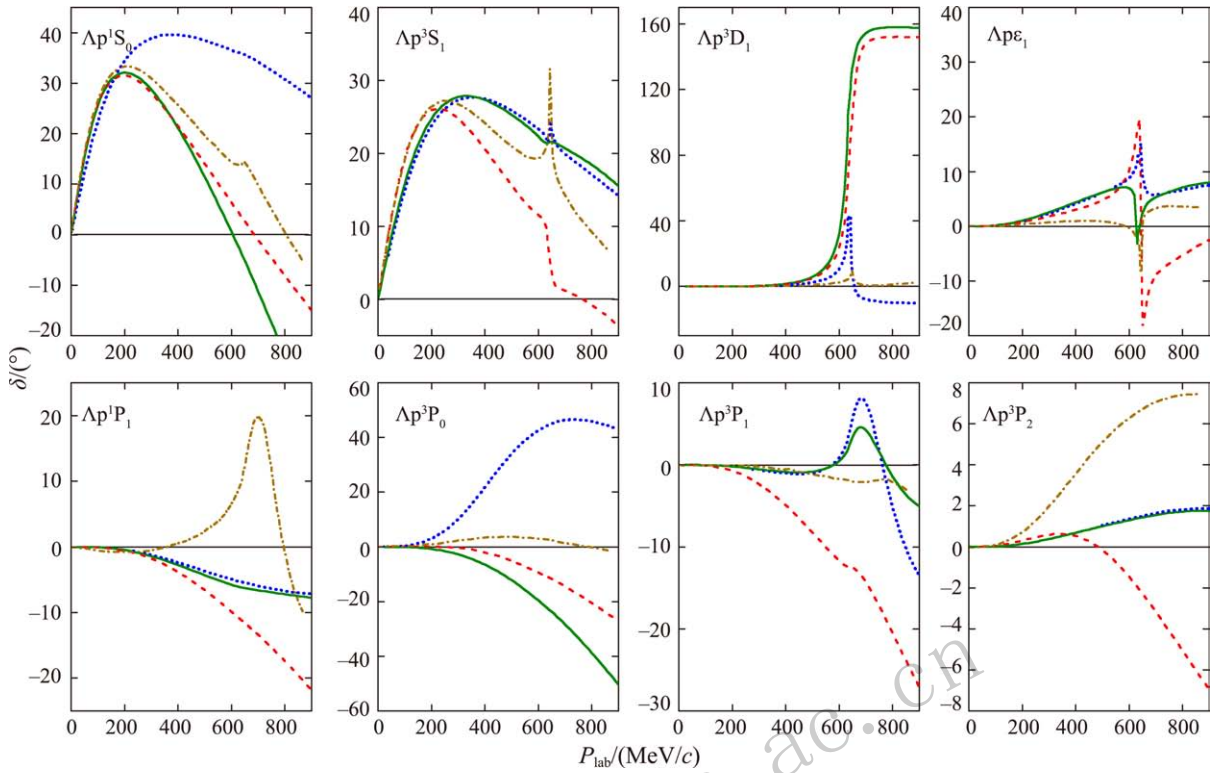

Fig. 8 (color online) Λp S- and P-wave phase shifts in the leading order relativistic ChPT approach (green solid lines) and NR approach (blue dotted lines) as functions of the laboratory momentum at $\Lambda_F = 600$ MeV. For reference, the NSC97f [11] (red dash lines) and Jülich 04[12] (orange dashed-dotted lines) results are also shown. The figure is taken from Ref. [46].

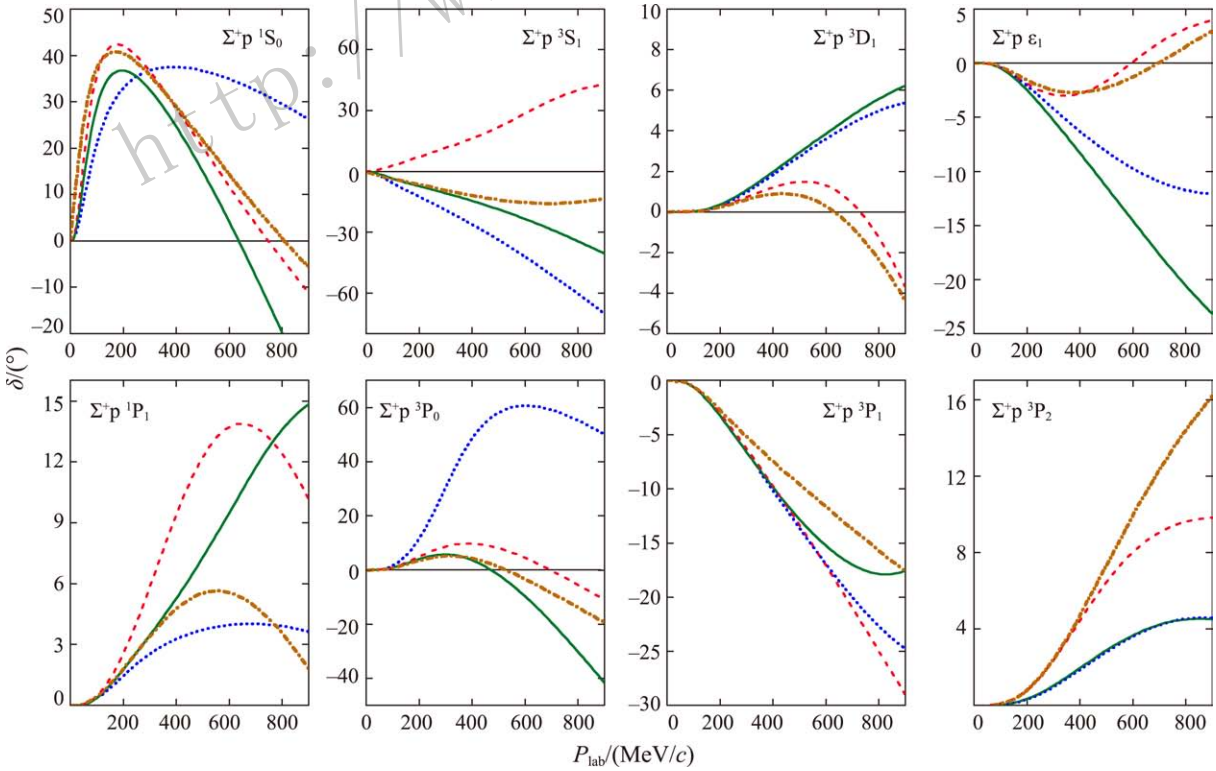

Fig. 9 (color online) Σ^+p S- and P-wave phase shifts in various approaches. The notations are the same as in Fig. 8. The figure is taken from Ref. [46].

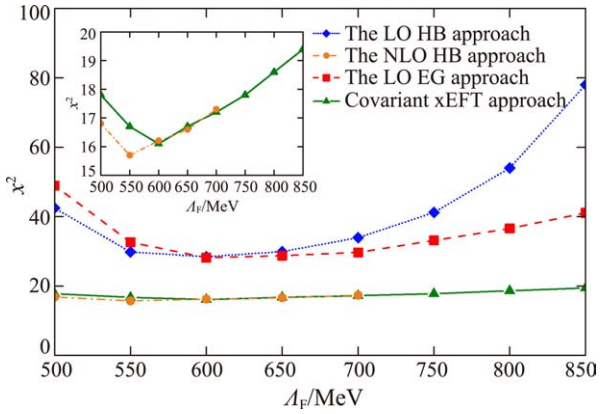

Fig. 10　(color online) χ^2 as a function of the cutoff in the LO (blue dotted line)[24], NLO (orange dashed-dotted line)[26] NR approach, the LO EG approach (red dashed line)[54] and the LO relativistic χEFT approach (green solid line).

the corresponding low energy constants and therefore study the impact of these interactions on various topics of current interests, such as the existence of exotic hadrons and the mass-radius relation of neutron stars.

References:

[1] BEANE S R, DETMOLD W, ORGINOS K, *et al.* Prog Part Nucl Phys, 2011, **66**: 1.

[2] AOKI S, DOI T, HATSUDA T, *et al.* [HAL QCD Collaboration]. PTEP, 2012, **2012**:01A105.

[3] DOI T, AOKI S, GONGYO S, *et al.* arXiv:1702.01600 [hep-lat].

[4] SASAKI K, AOKI S, DOI T, *et al.* arXiv:1702.06241 [hep-lat].

[5] ISHII N, AOKI S, DOI T, *et al.* arXiv:1702.03495 [hep-lat].

[6] YUKAWA H. Proc Phys Math Soc Jap, 1935, **17**: 48; [Prog Theor Phys 1935, **1**(Suppl.): 1.

[7] STOKS V G J, KLOMP R A M, TERHEGGEN C P F, *et al.* Phys Rev C, 1994, **49**: 2950.

[8] WIRINGA R B, STOKS V G J, SCHIAVILLA R. Phys Rev C, 1995, **51**: 38.

[9] MACHLEIDT R. Adv Nucl Phys, 1989, **19**:189.

[10] MACHLEIDT R. Phys Rev C, 2001, **63**: 024001.

[11] RIJKEN T A, STOKS V G J, YAMAMOTO Y. Phys Rev C, 1999, **59**: 21.

[12] HAIDENBAUER J, MEIßNER U G. Phys Rev C, 2005, **72**: 044005.

[13] WEINBERG S. Physica A, 1979, **96**: 327.

[14] WEINBERG S. Phys Lett B, 1990, **251**: 288.

[15] WEINBERG S. Nucl Phys B, 1991, **363**: 3.

[16] BEDAQUE P F, VAN KOLCK U. Ann Rev Nucl Part Sci, 2002, **52**: 339.

[17] ENTEM D R, MACHLEIDT R. Phys Rev C, 2003, **68**: 041001.

[18] EPELBAUM E, GLOCKLE W, MEIßNER U G. Nucl Phys A, 2005, **747**: 362.

[19] EPELBAUM E, HAMMER H W, MEIßNER U G. Rev Mod Phys, 2009, **81**: 1773.

[20] MACHLEIDT R, ENTEM D R. Phys Rept, 2011, **503**: 1.

[21] EPELBAUM E, KREBS H, MEIßNER U G. Phys Rev Lett, 2015, **115**: 122301.

[22] KANG X W, HAIDENBAUER J, MEIßNER U G. JHEP, 2014, **1402**: 113.

[23] DAI L Y, HAIDENBAUER J, MEIßNER U G. arXiv: 1702.02065 [nucl-th].

[24] POLINDER H, HAIDENBAUER J, MEIßNER U G. Nucl Phys A, 2006, **779**: 244.

[25] HAIDENBAUER J,MEIßNER U G,NOGGA A, *et al.* Lect Notes Phys, 2007, **724**: 113.

[26] HAIDENBAUER J, PETSCHAUER S, KAISER N, *et al.* Nucl Phys A, 2013, **915**: 24.

[27] POLINDER H, HAIDENBAUER J, MEIßNER U G. Phys Lett B, 2007, **653**: 29.

[28] HAIDENBAUER J, MEIßNER U G. Phys Lett B, 2010, **684**: 275.

[29] HAIDENBAUER J,MEIßNER U G, Petschauer S. Nucl Phys A, 2016, **954**: 273.

[30] SCHWERDTFEGER P. Relativistic Electronic Structure Theory, Part I. Fundamentals, Theoretical and Computational Chemistry Vol. 11[M]. Amsterdam: Elsevier Science Press, 2002.

[31] MENG J. Relativistic Density Functional for Nuclear Structure, International Review of Nuclear Physics Vol. 10[M]. Singapore: World Scientific, 2016.

[32] LIANG H, MENG J, ZHOU S G. Phys Rept, 2015, **570**: 1.

[33] GENG L S, MARTIN CAMALICH J, ALVAREZ-RUSO L, *et al.* Phys Rev Lett, 2008, **101**: 222002.

[34] GENG L S, MARTIN CAMALICH J, VICENTE VACAS M J. Phys Rev D, 2009, **79**: 094022.

[35] GENG L S, REN X L, MARTIN-CAMALICH J, *et al.* Phys Rev D, 2011, **84**: 074024.

[36] REN X L, GENG L S, MARTIN CAMALICH J, *et al.* JHEP, 2012, **1212**: 073.

[37] REN X L, GENG L S, MENG J. Phys Rev D, 2015, **91**: 051502.

[38] REN X L, ALVAREZ-RUSO L, GENG L S, *et al.* Phys Lett B, 2017, **766**: 325.

[39] GENG L S, KAISER N, MARTIN-CAMALICH J, *et al.* Phys Rev D, 2010, **82**: 054022.

[40] GENG L S, ALTENBUCHINGER M, WEISE W. Phys Lett B, 2011, **696**: 390.

[41] ALTENBUCHINGER M, GENG L S, WEISE W. Phys Lett B, 2012, **713**: 453.

[42] LU J X, REN X L, GENG L S. Eur Phys J C, 2017, **77**: 94.

[43] SHEN S H, HU J, LIANG H, *et al.* Chin Phys Lett, 2016, **33**(10): 102103.

[44] SHEN S, LIANG H, MENG J, *et al.* Phys Rev C, 2017, **96**: 014316.

[45] REN X L, LI K W, GENG L S, *et al.* arXiv:1611.08475 [nucl-th].

[46] LI K W, REN X L, GENG L S, *et al.* arXiv:1612.08482 [nucl-th].

[47] PARTOVI M H, LOMON E L. Phys Rev D, 1970, **2**: 1999.
[48] ERKELENZ K. Phys Rept, 1974, **13**: 191. doi: 10.1016/0370-1573(74)90008-8.
[49] BLANKENBECLER R, SUGAR R. Phys Rev,1966, **142**: 1051.
[50] THOMPSON R H. Phys Rev D, 1970, **1**: 110.
[51] KADYSHEVSKY V G. Nucl Phys B, 1968, **6**: 125.
[52] GROSS F. Phys Rev, 1968, **186**: 1448.
[53] EPELBAUM E, GEGELIA J. Phys Lett B, 2012, **716**: 338.
[54] LI K W, REN X L, GENG L S, *et al.* Phys Rev D, 2016, **94**: 014029.
[55] GIRLANDA L, PASTORE S, SCHIAVILLA R, *et al.* Phys Rev C, 2010, **81**: 034005. doi: 10.1103/Phys Rev C.81.034005 [arXiv:1001.3676 [nucl-th]].
[56] DJUKANOVIC D, GEGELIA J, SCHERER S, *et al.* Few Body Syst, 2007, **41**: 141.
[57] PETSCHAUER S, KAISER N. Nucl Phys A, 2013, **916**: 1.
[58] STOKS V G J, KLOMP R A M, RENTMEESTER M C M, *et al.* Phys Rev C, 1993, **48**: 792.
[59] EPELBAUM E, GLOECKLE W, MEIßNER U G. Nucl Phys A, 2000, **671**: 295.
[60] ARNDT R A, STRAKOVSKY I I, WORKMAN R L. Phys Rev C, 1994, **50**: 2731.
[61] DE SWART J J. Rev Mod Phys, 1963, **35**: 91; Erratum: Rev Mod Phys, 1968, **37**: 326.

基于手征微扰理论构建相对论重子-重子相互作用

任修磊[1]，李凯文[2]，耿立升[2,3,†]

(1. 北京大学物理学院，核物理与核技术国家重点实验室；北京 100871；
2. 北京航空航天大学物理科学与核能工程学院&宇宙中的核物理交叉研究中心；北京 100191；
3. 先进核能材料与物理北京市重点实验室；北京 100191)

摘要： 介绍了两个近期基于协变手征微扰理论构建领头阶核子-核子和超子- 核子相互作用的工作。理论中未知的低能常数通过拟合核子-核子和超子-核子散射实验数据确定。分析发现，在对散射数据的描述上，领头阶相对论手征力可以媲美次领头阶非相对论手征核力。研究表明，构建相对论手征重子-重子相互作用技术上是可行的。得到的相互作用不仅可以为相对论核结构及反应研究提供重要的理论输入，而且可以进一步加深对低能强相互作用的认识。

关键词： 核子-核子相互作用；超子-核子相互作用；协变手征微扰理论

收稿日期： 2017-03-19； **修改日期：** 2017-05-20
基金项目： 国家自然科学基金资助项目 (11375024, 11522539, 11735003, 11335002, 11621131001)；中国博士后科学基金项目 (2016M60084, 2017T100008).
† **通信作者：** 耿立升，E-mail: lisheng.geng@buaa.edu.cn .